PHYSICAL REVIEW B **71**, 140502(R) (2005)

Vortex-state-dependent phase boundary in mesoscopic superconducting disks

B. J. Baelus,[1,2,*] A. Kanda,[3,†] F. M. Peeters,[2] Y. Ootuka,[3] and K. Kadowaki[1]
[1]*Institute of Materials Science, University of Tsukuba, Tsukuba 305-8573, Japan*
[2]*Departement Fysica, Universiteit Antwerpen (Campus Drie Eiken), Universiteitsplein 1, B-2610 Antwerpen, Belgium*
[3]*Institute of Physics and Tsukuba Research Center for Interdisciplinary Material Science (TIMS), University of Tsukuba, Tsukuba 305-8571, Japan*
(Received 18 January 2005; published 8 April 2005)

The temperature dependence of the vortex penetration and expulsion fields in mesoscopic superconducting disks are studied. We experimentally find that the penetration field decreases with increasing temperature for all values of the vorticity. On the other hand, the temperature dependence of the expulsion fields shows two regimes: For some vortex states the expulsion field increases with temperature, while for other states it is almost temperature independent. A numerical study based on the nonlinear Ginzburg-Landau theory confirms that the former regime corresponds to multivortex states and the latter to giant vortex states. The origin of this difference is discussed.

DOI: 10.1103/PhysRevB.71.140502 PACS number(s): 74.78.−w, 74.62.−c, 74.25.Fy

Mesoscopic superconducting disks have sizes comparable to the superconducting coherence length ξ and/or the magnetic penetration depth λ. Because of the small sample size, the vortex configuration in such disks is different from the triangular Abrikosov lattice, the lowest energy configuration in bulk type-II superconductors. The competition between the vortex-vortex interaction and the boundary that tries to impose its symmetry determines the (meta)stable vortex configurations.

During the last decade, vortex states in mesoscopic disks attracted a lot of attention, both theoretically[1–6] and experimentally.[7–10] Theoretically, it was predicted that two possible vortex states are stable in mesoscopic superconducting disks. In a giant vortex state (GVS) the order parameter has a single zero with a winding number L (also called vorticity).[1] For superconducting disks, the GVS is circular symmetric. On the other hand, the multivortex state (MVS) is the finite-size version of the Abrikosov lattice, deformed by the boundary of the sample. For example, vortices are arranged in rings in small superconducting disks.[2]

Conventional experiments on mesoscopic superconductors have measured the resistivity[9,10] and the magnetization[7,8] of the different vortex states. Since these experiments do not provide any information on the vortex positions, for a long time there was no direct experimental proof for the existence of the two possible vortex states in mesoscopic disks. Recently Kanda *et al.* developed the multiple-small-tunnel-junction (MSTJ) method, in which multiple small tunnel junctions with high tunnel resistance are attached to a mesoscopic superconductor in order to detect small changes in the local density of states (LDOS) under the junctions.[11–13] The LDOS depends on the local supercurrent density, so the MSTJ method provides information on the supercurrent. It was shown that with this MSTJ method, one obtains information on the symmetry of the vortex configuration that allowed us to distinguish experimentally the MVS from the GVS in mesoscopic superconducting disks.[14]

In this paper, we present data on the temperature dependence of the vortex penetration and expulsion fields for the same sample as reported in Ref. 14, along with the results of theoretical simulations based on the nonlinear Ginzburg-Landau (GL) theory. While, in Ref. 14, we focused on the direct experimental distinction between MVSs and GVSs, we present here a remarkable difference in the temperature dependence of the expulsion fields between the MVSs and GVSs. Since the transition fields can be obtained by different existing experimental techniques [e.g., ballistic Hall magnetometry and superconducting quantum interference device (SQUID) magnetometry], this method might provide a very powerful tool for obtaining information about MVSs and GVSs by conventional techniques.

A schematic drawing of the experimental sample is shown in the inset of Fig. 1(a). Four normal metal (Cu) leads are connected to the periphery of a superconducting Al disk through highly resistive small tunnel junctions *A*, *B*, *C*, and *D*. The disk radius was 0.75 μm and the thickness was 33 nm. The disk was directly connected to an Al drain lead. The coherence length ξ_0 was 0.15 to 0.19 μm and the superconducting transition temperature T_c was 1.3–1.4 K. In the measurement, the voltage at a fixed current of 100 pA over each junction was measured as a function of the applied magnetic field perpendicular to the disk. Comparison of voltages at symmetrical positions (*A* and *D*, or *B* and *C*) allows us to estimate the vortex configurations. Details of the experiment are described in Ref. 14.

Figure 1(a) shows the voltage of junction *D* as a function of the applied magnetic field at temperature values $T=0.1$ (highest curve), 0.2, 0.3, 0.4, and 0.5 K (lowest curve) for decreasing external field. The jumps correspond to the expulsion of a single vortex. The numbers in the figure indicate the vorticity. At low fields the expulsion fields are almost independent of temperature, while at higher fields they increase with increasing temperature. This can be clearly seen from the square symbols that indicate the $L=5\rightarrow4$ and the $L=13\rightarrow12$ transition fields. Figure 1(b) shows the same as Fig. 1(a) but now for increasing field. The penetration fields, given by the peaks in the voltage, always decrease with increasing temperature.

To investigate the origin of these behaviors, we calculated the lowest free energy for the vortex states in a mesoscopic

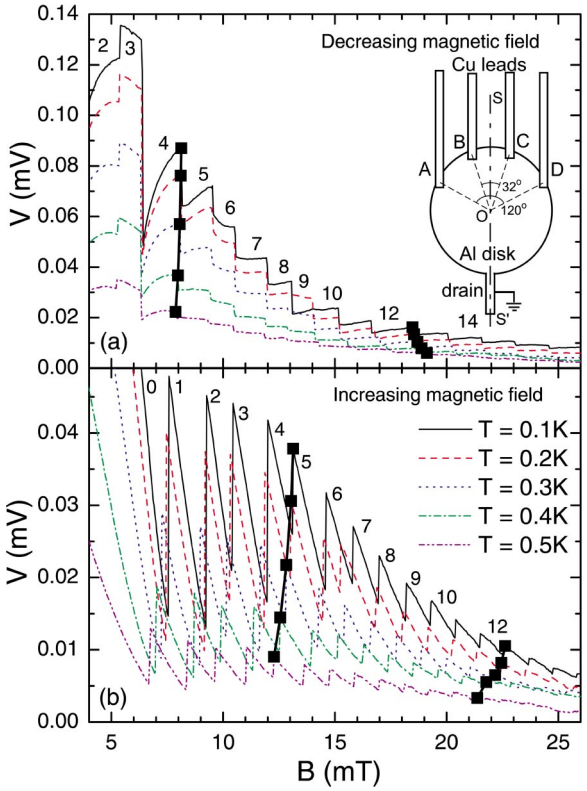

FIG. 1. (Color online) The voltage of junction D as a function of the applied magnetic field when (a) decreasing or (b) increasing the field for several values of the temperature, i.e., $T=0.1$ (highest curve), 0.2, 0.3, 0.4, and 0.5 K (lowest curve). The current through the junction was 100 pA. The square symbols indicate the transitions fields between the states with $L=4$ and 5, and $L=12$ and 13. The inset in (a) shows schematically the experimental sample.

superconducting disk within the framework of the nonlinear GL theory. This theoretical analysis is based on a full self-consistent numerical solution of the coupled GL equations, taking into account the demagnetization effects. A more detailed description of the theoretical model can be found in Refs. 1 and 2. The parameters were chosen in such a way that they correspond to the experimental sample, i.e., radius $R=5.0\xi$, thickness $d=0.1\xi$, and the GL parameter $\kappa=0.28$.

Figure 2 shows the free energy as a function of the applied magnetic field when decreasing the field for several values of the temperature, i.e., $T=0.1$ (lowest curve), 0.2, 0.3, 0.4, and 0.5 K (highest curve). Notice that at low fields the transition fields are almost independent of temperature, while at high fields the transition fields increase with increasing temperature, in agreement with the experimental observation. The inset shows the free energy for the same values of the temperature when increasing the applied magnetic field. Each jump corresponds to the penetration of one vortex. It is clear that the penetration fields always decrease with increasing temperature, also in agreement with the experiment.

To compare the theoretical and the experimental results in more detail, we show in Fig. 3 the penetration and expulsion fields as a function of temperature both as calculated within the GL theory, and observed by using the MSTJ method. The

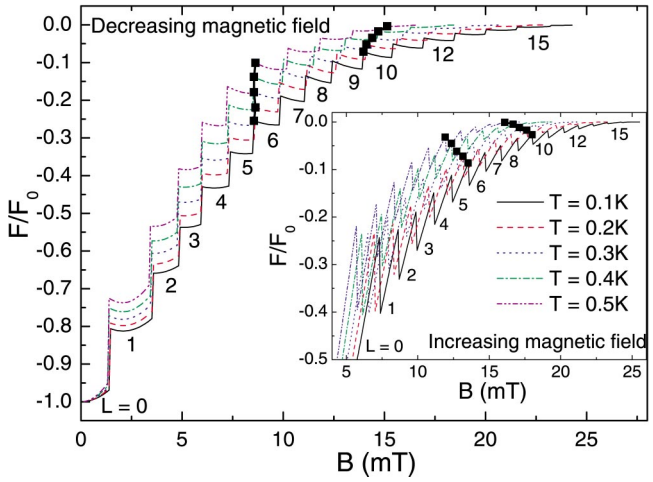

FIG. 2. (Color online) The free energy for a superconducting disk with $R=5.0\xi$, $d=0.1\xi$, and $\kappa=0.28$ as a function of the applied magnetic field when decreasing the field for several values of the temperature, i.e., $T=0.1$ (lowest curve), 0.2, 0.3, 0.4, and 0.5 K (highest curve). The inset shows the same when the field is increased. The square symbols indicate the transition fields between the states with $L=5$ and 6, and $L=9$ and 10.

numbers in the figure give the vorticity of the vortex state before the transition. All the penetration fields decrease with temperature [Figs. 3(a) and 3(c)]. The magnetic field interval between the different transitions is almost constant and decreases slightly with increasing temperature. In the experiment, the slope is smaller for lower temperatures, which is not the case in the theory. This discrepancy is presumably due to the heating effect caused by the current flowing through the junctions.

The behavior of the expulsion fields as a function of the temperature is more interesting [see Fig. 3(b)]. For small values of the vorticity, the theoretically obtained expulsion field is almost constant (in fact, they decrease very slightly with increasing temperature), while for higher vorticity, e.g., $L=8$, we see that the transition fields are constant for low temperatures and increase with temperature at higher temperatures. For the highest values of the vorticity, the transition fields always increase with temperature. The experimentally obtained expulsion fields have the same features as shown in Fig. 3(d).

What determines the behavior of the expulsion fields? From the theoretical calculations, it becomes clear that the type of the vortex state (MVS or GVS) just before the transition determines the temperature dependence. From Fig. 3(b) we see that the expulsion fields are almost independent of the temperature when the last state is a MVS (indicated by the closed symbols), and increase with temperature when the last state is a GVS (indicated by the open symbols). Experimentally, the boundary of the two behaviors at low temperatures is between $L=11$ and 12 [Fig. 3(d)]. From the MSTJ measurement, we know that at 0.03 K the MVS appears for $L=2$–11 and the GVS for $L\geqslant 12$ in decreasing fields.[14] Assuming that the vortex configuration at 0.03 K is the same as that at 0.1 K,[15] the experimental results indicate that the two kinds of temperature dependence correspond to the MVSs and the GVSs, in agreement with the theory.

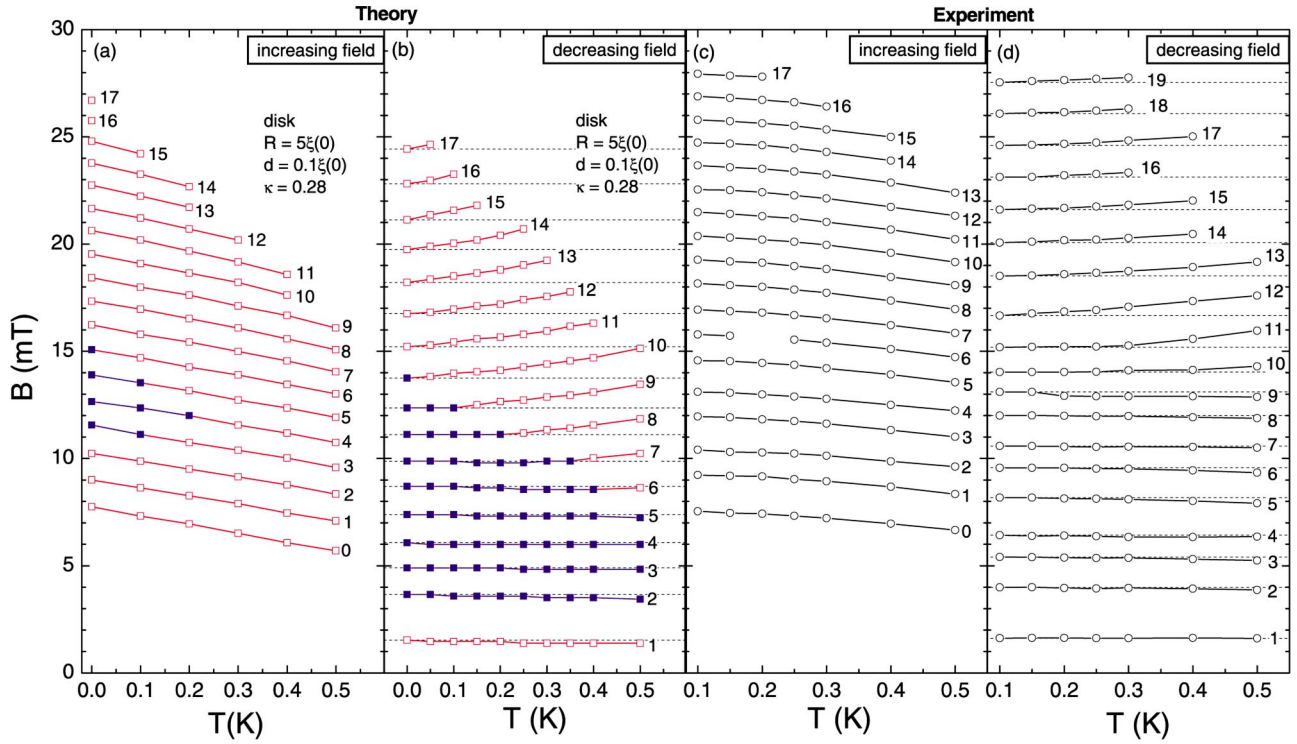

FIG. 3. (Color online) The theoretical and experimental penetration and expulsion fields as a function of the temperature; (a) the theoretical $L \rightarrow L+1$ penetration fields, (b) the theoretical $L \rightarrow L-1$ expulsion fields, (c) the experimental $L \rightarrow L+1$ penetration fields, and (d) the experimental $L \rightarrow L-1$ expulsion fields. The dashed lines correspond to the values of the expulsion field at the lowest temperature and are guides to the eye. The closed symbols in (a) and (b) correspond to a MVS and open symbols to a GVS just before the transition.

Why is the temperature dependence of the expulsion fields different for the MVSs and the GVSs? The expulsion fields of the vortices are determined by the surface barrier, which decreases with decreasing field (at least close to the expulsion field). At the expulsion field the barrier becomes sufficiently low such that one vortex can leave the sample. The surface barrier originates from the superconducting currents flowing near the edge of the sample. Thus, to investigate the different temperature dependences of the expulsion fields for MVSs and GVSs, it is necessary to study the superconducting current distribution near the disk boundary in more detail. From the local values for the order parameter Ψ and the vector potential $\vec{A}$ obtained from the self-consistent solution of the GL equations, we calculate the local superconducting current $\vec{j}=(\Psi^*\vec{\nabla}\Psi-\Psi\vec{\nabla}\Psi^*)/2i-|\Psi|^2\vec{A}$.

The upper curves in Fig. 4 are the radial dependence of the supercurrent calculated for the GVS with $L=11$, for $T=0.1$, 0.2, 0.3, and 0.4 K. The magnetic field is chosen just above the $L=11 \rightarrow 10$ expulsion field for $T=0.4$ K. In the center, the supercurrent is zero at the position of the GVS with $L=11$. Around this vortex "positive" currents (i.e., clockwise direction) are flowing and near the edge are "negative" screening currents (i.e., counterclockwise direction). The competition of these two currents leads to a zero current density at a certain radial position ρ^*, which is independent of temperature and is determined such that the flux ϕ corresponding to the external field through an area with radius ρ^* is exactly L times the flux quantum ϕ_0, i.e., $\phi=B\pi(\rho^*)^2=11\phi_0$. From Fig. 4 it is clear that the size of the current near the boundary decreases (or becomes less negative) with increasing temperature. Therefore, the surface barrier decreases with increasing temperature and a vortex will be expelled at higher fields. As a consequence, for a GVS the expulsion field increases with increasing temperature.

The lower curves in Fig. 4 show the radial dependence of the supercurrent for the MVS with $L=4$ for the same values of the temperature at $B=6.1$ mT, which is just above the expulsion field. In the case of a MVS, the current is no longer circular symmetric and therefore we took the direc-

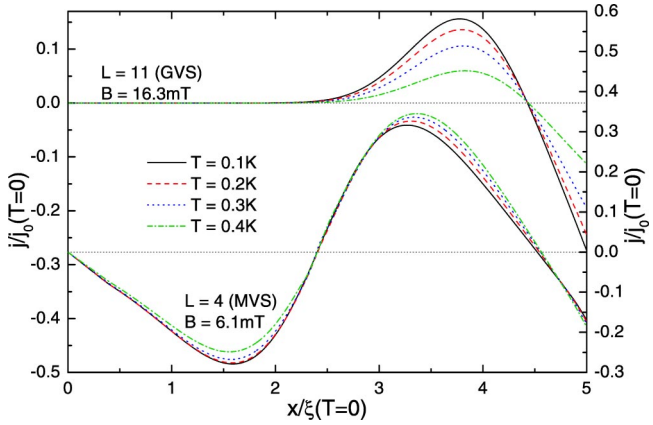

FIG. 4. (Color online) The radial dependence of the current density for the GVS with $L=11$ and the MVS with $L=4$ for several values of the temperature. For the MVSs the radial direction is taken through one of the vortex cores.

tion through one of the vortex cores in Fig. 4. The four vortices are situated on a circle at a distance $x=2.4\xi$ from the disk center. We found that the position of the vortex is independent of temperature. The current flowing around the vortex results in negative currents towards the inside and positive currents towards the outside. At the disk center, no vortex is situated, although the total current is zero. The reason is that the currents flowing around the four vortices compensate each other in this point. Near the outside of the disk, a negative screening current is flowing. It is important to notice that the current near the disk edge is almost temperature independent. This leads to a surface barrier and therefore also to an expulsion field that are almost temperature independent. Looking more carefully, it is clear that the current near the edge becomes slightly more negative with increasing temperature. This explains why the expulsion fields slightly decrease with increasing temperature when the state is a MVS.

Although there is good qualitative agreement, the quantitative agreement between theory and experiment is not perfect (see Fig. 3). The main reason is that the zero-temperature value of the coherence length ξ_0 and the zero-field critical temperature T_c is not so well defined experimentally, while theoretically these parameters influence the results drastically, since all sizes are in units of $\xi(T)$, which depends on ξ_0 and T_c. Furthermore, we assumed $\xi(T)=\xi_0/\sqrt{1-T/T_c}$, which may not be exactly valid in the whole temperature region. Other reasons for the difference between theory and experiment are that the experimental sample may contain defects, which favor the MVS above the GVS (see also Ref. 14) and that a small heating effect may be present due to the tunnel current. However, a perfect quantitative agreement is beyond the scope of the present article.

In conclusion, we found that the temperature dependence of the vortex expulsion fields is closely related to the vortex states in mesoscopic superconducting disks. There is a close agreement between the theoretical results obtained by solving the GL equations, and the experimental results, by measuring the voltage using the MSTJ method. Although further intensive study on shape and size dependence is needed, the present results indicate that the temperature dependence of the vortex expulsion fields becomes a powerful tool to identify the vortex states such as MVSs and GVSs.

This work was supported by the University of Tsukuba Nanoscience Special Project, the 21st Century COE Program of MEXT, the Flemish Science Foundation (FWO-Vl), and the Belgian Science policy. B. J. B. acknowledges support from JSPS and FWO-Vl.

*Email address: ben.baelus@ua.ac.be

†Email address: kanda@lt.px.tsukuba.ac.jp

[1] V. A. Schweigert and F. M. Peeters, Phys. Rev. B **57**, 13817 (1998).

[2] V. A. Schweigert, F. M. Peeters, and P. S. Deo, Phys. Rev. Lett. **81**, 2783 (1998).

[3] J. J. Palacios, Phys. Rev. B **58**, R5948 (1998).

[4] J. J. Palacios, Phys. Rev. Lett. **84**, 1796 (2000).

[5] B. J. Baelus, L. R. E. Cabral, and F. M. Peeters, Phys. Rev. B **69**, 064506 (2004).

[6] L. R. E. Cabral, B. J. Baelus, and F. M. Peeters, Phys. Rev. B **70**, 144523 (2004).

[7] A. K. Geim, I. V. Grigorieva, S. V. Dubonos, J. G. S. Lok, J. C. Maan, A. E. Filippov, and F. M. Peeters, Nature (London) **390**, 256 (1997).

[8] A. K. Geim, S. V. Dubonos, I. V. Grigorieva, K. S. Novoselov, F. M. Peeters, and V. A. Schweigert, Nature (London) **407**, 55 (2000).

[9] V. V. Moshchalkov, L. Gielen, C. Strunk, R. Jonckheere, X. Qiu, C. Van Haesendonck, and Y. Bruynseraede, Nature (London) **373**, 319 (1995).

[10] V. Bruyndoncx, L. Van Look, M. Verschuere, and V. V. Moshchalkov, Phys. Rev. B **60**, 10468 (1999).

[11] A. Kanda, M. C. Geisler, K. Ishibashi, Y. Aoyagi, and T. Sugano, in *Quantum Coherence and Decoherence ISQM-Tokyo '98*, edited by Y. A. Ono and K. Fujikawa (Elsevier, Amsterdam, 1999), p. 229.

[12] A. Kanda and Y. Ootuka, Microelectron. Eng. **63**, 313 (2002).

[13] A. Kanda and Y. Ootuka, Physica C **404**, 205 (2004).

[14] A. Kanda, B. J. Baelus, F. M. Peeters, K. Kadowaki, and Y. Ootuka, Phys. Rev. Lett. **93**, 257002 (2004).

[15] This assumption seems to be reasonable because the measured transition points at 0.03 K are about the same as those at 0.1 K, presumably due to the heating effect caused by the current flowing through the junctions.